

11,04

Phase transitions in frustrated cobaltite  $\text{TmBaCo}_4\text{O}_7$ 

© Z.A. Kazei, V.V. Snegirev, M.S. Stolyarenko

Moscow State University,  
Moscow, Russia

E-mail: kazei@plms.phys.msu.ru

Received July 3, 2023

Revised August 3, 2023

Accepted August 4, 2023

For the first time, changes in lattice parameters (metrics) during a structural transition in stoichiometric cobaltite  $\text{TmBaCo}_4\text{O}_{7+x}$  with  $x \approx 0$  (iodometric titration method) obtained by quenching from 900–950°C were investigated by direct X-ray method. It was found that during the structural transition  $T_S \approx 220$ –240 K, the  $\Delta a/a$  parameter does not detect any features, parameters  $b$  and  $c$  experience jumps of different sign and different magnitude  $\Delta b/b \approx 3.5 \cdot 10^{-3}$  and  $\Delta c/c \approx -4.0 \cdot 10^{-3}$ , which leads to a jump in the volume of  $\Delta V/V \approx -0.5 \cdot 10^{-3}$ . The distortion value  $\varepsilon_o \approx -3.5 \cdot 10^{-3}$  remains constant with increasing temperature and disappears abruptly during the transition. The distortion of the structure is accompanied by anomalous behavior of the Young's modulus  $\Delta E(T)/E_0$  in the  $T_S$  region. In the region of the expected magnetic phase transition of the cobalt subsystem, anomalies in the Young's modulus curve  $\Delta E(T)/E_0$  were not detected, and a strong absorption peak at  $T \approx 96$  K in the internal friction dependence  $q^{-1}(T)$  is, apparently, a sign of a developed short-range order.

**Keywords:** frustrated systems, cobaltites, structural phase transitions, lattice parameters, isotropic deformation, anisotropic deformation, Young's modulus, internal friction.

DOI: 10.61011/PSS.2023.09.57119.138

## 1. Introduction

Geometrically frustrated systems have been a target of numerous experimental and theoretical investigations in recent years [1,2]. The most extensively studied systems are antiferromagnetic materials with the Kagome lattice and pyrochlore structure that have disordered ground states [3,4]. It was shown that various weak perturbation in these systems such as small distortions of structure, interactions with the next nearest neighbors, magnetic anisotropy, etc., may reduce the ground state degeneracy and promote the occurrence of a long-range magnetic order.

Layered cobaltites  $\text{RBaCo}_4\text{O}_{7+x}$  (variable  $x$  means deviation from stoichiometry by oxygen) are of particular interest, because they have alternating linked triangular layers and Kagome layers at the same time in their structure. After discovery of layered cobaltite  $\text{YBaCo}_4\text{O}_{7+x}$ , cation substitutions have been used to synthesize a family of rare-earth (RE) isomorphous  $\text{RBaCo}_4\text{O}_{7+x}$  compounds with heavy RE ions and Ca. These compounds demonstrate wide versatility of interesting physical and structural properties provided by the combination of mixed valence of cobalt and frustrated triangular lattice and Kagome lattice in their structure [5–12].

Frustrations occur in the system, when it is impossible to satisfy simultaneously the minimum energy of pairwise interactions in bypassing a closed chain with an arbitrary number of spins. They occur in the chain, for which the product of spin-spin interaction constants along the chain is negative. Thus, frustrations are the consequence of particular topology of the crystal structure (geometrical

frustrations) and often result in the system ground state degeneracy [13]. The simplest example is a frustrated system of three spins with negative spin-spin interaction constants of the same modulus  $J_{ij}$ .

RE cobaltites allow to study the fundamental problems of solid-state and magnetism physics such as nontrivial ground states, features of phase transitions and short-range order effects in the presence of frustrated and competing exchange interactions, spin crossover, metal–dielectric transition, etc. In addition,  $\text{YBaCo}_4\text{O}_7$  and its derivatives exhibit high chemical mobility demonstrating the reversible oxygen absorption and desorption capability [14–16]. Using the super-high pressure for oxygenation, a record-high excess oxygen with  $x \approx 1.56$  for  $\text{YBaCo}_4\text{O}_{7+x}$  was achieved [17] that exceeded the known parameters for other oxide materials.

Stoichiometric compounds with the  $\text{R}^{3+}$  trivalent ion contain mixed valence cobalt ions  $\text{Co}^{2+}$  and  $\text{Co}^{3+}$  at the ratio of 3:1, which are randomly distributed in the structure over two types of tetrahedral sites. The ratio of aliovalent  $\text{Co}^{2+}/\text{Co}^{3+}$  ions in a cobalt subsystem can be varied using non-isovalent substitution  $\text{R}^{3+} \rightarrow \text{Ca}^{2+}$  or  $\text{Co}^{2+}/\text{Co}^{3+} \rightarrow \text{Zn}^{2+}/\text{Al}^{3+}$ , as well as by varying oxygen content ( $7+x$ ).

Crystalline structure of RE-cobaltites at high temperatures is described by a hexagonal  $P6_3mc$  space group [18–20] (in some publications, trigonal space group  $P31c$  is used [21,22]). In the framework crystal structure, the corner-sharing  $\text{CoO}_4$  tetrahedra form triangular layers and Kagome layers alternatively packed along the  $c$  axis. Larger octahedral and cuboctahedral sites in a three-dimensional tetrahedral network are occupied by  $\text{R}^{3+}$  and

$Ba^{2+}$  cations, respectively. In an infinite flat lattice of linked triangles, frustrations in the magnetic system result in the degenerate ground state and the absence of long-range magnetic order even at considerably high exchange interaction constants [13]. A small distortion of structure in stoichiometric RE-cobaltites removes the frustration of exchange interactions promoting the development of a long-range magnetic order in the Co subsystem below the structural transition temperature  $T_S$  [23–26].

Y — the cobaltite containing one type of magnetic ions undergoes the structural transition at  $T_S = 313$  K resulting in decreasing symmetry from hexagonal to orthorhombic (space group  $Pbn2_1$ ;  $a_o \approx a_h$ ,  $b_o \approx \sqrt{3}a_h$ ), and is followed by anomalies of elastic, magnetic and transport properties. Critical structural transition temperature  $T_S$  of cobaltites with magnetic RE ions decreases steadily with decreasing RE ion radius [27–30]. Below the structural transition in  $YBaCo_4O_7$  a three-dimensional antiferromagnetic ordering occurs in the Co subsystem at  $T_N \approx 110$  K resulting in lower monoclinic  $P112_1$  symmetry [5,13,31]. With further temperature decrease, another magnetic phase transition is observed at  $T_{N2} \sim 70$  K [32], which is attributable to the spin reorientation in the Co subsystem [13]. Due to the frustration of exchange interactions, the long-range magnetic order is established at a temperature that is considerably lower than the paramagnetic temperature  $\theta_{CW} = -508$  K and is characterized by a complex noncollinear magnetic structure [5,13].

The RE cobaltite structure is studied in sufficient detail for the hexagonal phase and much less studied for the distorted orthorhombic phase. Behavior of lattice constants (lattice metric) during the structural transition, as well as transition temperature and distortion variation with different substitutions in Co and RE sublattices or deviation from stoichiometry are understudied. Lattice constant behavior during the structural transition and change of this behavior in case of deviation from stoichiometry are studied in [25,26,30,33]. Investigations of the  $YBaCo_4O_{7+x}$  system have shown that at a small deviation from stoichiometry the structure is still undistorted hexagonal, frustrations are maintained and, therefore, magnetic transition in the Co subsystem is quickly diffused (if any long-range magnetic order transition is still present at all) [25]. The effect of structure distortion on the frustrated Co subsystem behavior was studied for a series of Y-cobaltites with small deviation from stoichiometry. In particular, elastic and magnetic properties of layered  $YBaCo_4O_{7+x}$  cobaltites have been found to be highly dependent upon excess oxygen [25]. Dependence of elastic and magnetic properties upon excess oxygen and interrelation of the structural and magnetic phase transitions were studied for  $DyBaCo_4O_{7+x}$  [34] and  $ErBaCo_4O_{7+x}$  cobaltites [26,35].

The objective of this study was to investigate structural and elastic properties of stoichiometric  $TmBaCo_4O_7$  cobaltite containing two types of magnetic ions and then to compare with stoichiometric  $YBaCo_4O_7$  cobaltite. The

effect of RE subsystem and its interaction with Co subsystem on phase transitions and physical properties in complex layered cobaltites are almost not studied. RE ion generally results in considerable magnetic anisotropy change, which, together with structure distortion, affects the establishment of long-range magnetic order in frustrated systems.

## 2. Samples and experiment technique

Polycrystalline  $TmBaCo_4O_7$  studied samples were synthesized using the ceramic process. For synthesis, we used oxides  $Tm_2O_3$ ,  $BaCO_3$  and  $Co_3O_4$  that had been previously annealed in air at 800, 400 and 700°C, respectively. The synthesis was carried out in air in three stages at 900, 1000 and 1100°C with intermediate grinding. Each stage was ended with sample annealing from 900–950°C, for which the heated sample was cooled abruptly to the liquid nitrogen temperature (for details see [36]). After the synthesis and annealing from 900–950°C, oxygen content in ceramic cobaltite samples is usually within  $x \sim 0.05–0.10$ , therefore, to achieve the required oxygen content and uniform oxygen distribution within the samples, the ceramic samples are additionally heat treated [37]. This paper describes the investigation of the „as prepared“  $TmBaCo_4O_7$  sample annealed from 900–950°C and not subjected to additional heat treatment. With additional heat treatment of cobaltites, oxygen content and distribution varies resulting in the change of degree and type of distortion of the structure and all physical properties. The influence of additional heat treatment on the physical properties of  $TmBaCo_4O_{7+x}$  requires separate study and is not discussed herein.

Oxygen content in the samples was measured by the iodometric titration, for which the sample was dissolved in acid solution followed by reduction of high-valent  $Co^{3+}$  with an appropriate reducing agent [25]. For this, two to three successive experiments were carried out, where  $\sim 30$  mg of the studied sample were solved in 1.5 M HCl solution containing excess KI. Reduction of high-valent  $Co^{3+}$  ions of the sample to  $Co^{2+}$  ions resulted in the formation of a stoichiometric quantity of iodine in the solution, which was titrated by 0.02 M  $Na_2S_2O_3$  solution metered by an electronic piston burette. The end-point of titration (equivalence point) was determined by measuring EMF jump in a reversible cell consisting of the indicating electrode (platinum electrode) and reference electrode (calomel electrode with double electrode junction) immersed in the test solution. The whole titration process was carried out using a software-controlled original automated system (see [26] for more details).

Iodometric titration of cobaltite samples with different RE ions has shown that oxygen content in the samples depends both on heat treatment and the type of RE ion. After the synthesis and annealing from 900–950°C,  $RBaCo_4O_{7+x}$  ceramics with Dy to Er ions usually have small excess oxygen and ceramics with heavier Tm–Lu ions are close to stoichiometric. In the annealed  $TmBaCo_4O_7$  cobaltite,

oxygen content is close to stoichiometric  $x \approx 0$ , and vacuum annealing results in oxygen deficiency of  $x \approx -0.06$ .

X-ray examinations at room temperature were carried out on polycrystalline powder samples using Stoe diffractometer with a monochromator on the primary beam ( $\text{CoK}\alpha_1$ -radiation). Temperature X-ray measurements were carried out using „Geigerflex“ (Japan) diffractometer with  $\text{CoK}\alpha$  radiation without monochromator and equipped with „Oxford\_Instruments“ (UK) continuous-flow cryostat to achieve and maintain the temperature with accuracy 0.1 K within the range of (77–300) K. The sample was attached to a cold finger cooled by nitrogen jet and placed in vacuum.

The Young modulus  $E(T)$  and internal friction coefficient  $q^{-1}(T)$  were measured by the composite resonator method at  $\sim 100$  kHz within the range of 80–280 K using an original automated system (see [30] for more details).

Single-crystal quartz and sample forming a composite resonator were attached using BF-2 adhesive with polymerization. The sample was a parallelepiped with cross-section  $2 \times 3$  mm and the length ( $\sim 10$ – $12$  mm) was chosen such that natural frequencies of the quartz and sample agree within  $\sim 5\%$ . If these frequencies are close to each other, then mechanical stresses in the glue splice are equal to zero and the adhesive effect may be ignored.

Temperature measurements were carried out in steady state (temperature measurement accuracy  $\pm 0.03$  K) and the temperature interval and holding time (at least 10–15 min) in the phase transition region varied within wide ranges to ensure stationarity.

### 3. Experimental findings and discussion

#### 3.1. X-ray diffraction analysis

Structural investigations of the  $\text{TmBaCo}_4\text{O}_7$  sample are also of interest in terms of detecting structure distortion that releases frustrations and for identifying the nature of structural transition in the RE cobaltite family. At room temperature, all X-ray pattern lines of the  $\text{TmBaCo}_4\text{O}_7$  studied sample were identified in terms of a hexagonal structure (Figure 1; the sample contained a small amount of  $\sim 3\%$  thulium oxide). The quality of describing an X-ray diffraction pattern may be assessed by parameter  $\chi^2 = 1.4$  the impurity line region from the sample holder and impurity phase was excluded).

With decreasing temperature structure distortion was observed and splitting of all lines in the X-ray pattern at  $T = 80$  K corresponds to a slightly distorted hexagonal structure with slight rhombic distortion. Full X-ray pattern in the cryostat with acceptable statistics is a time consuming process and, what is important, is not necessary to determine the structure parameters when symmetry has been already defined. In the temperature range from 80 K to  $T_S$ , the structure has been found to be still rhombic [13], and for temperature measurements of the parameters  $a$ ,  $b$  and  $c$  of the distorted lattice cell (designations for the rhombic

cell are used below), it is sufficient to measure dependences of three reflections on temperature.

Full-profile X-ray analysis of  $\text{TmBaCo}_4\text{O}_7$  has shown that at  $T = 80$  K the sample is distorted and its structure at low temperatures is described taking into account small rhombic distortion. In the temperature range from 80 K to  $T_S$ , the structure remains rhombic and it is sufficient for temperature measurements to study the dependences of three reflections on temperature. Distortion  $\varepsilon_o$  as well as cell parameters  $a$  and  $b$  were determined by one peak  $\{(400) + (260)\}$  that was split in case of distortion (Figure 2). For temperature measurements of the  $c$  parameter, reflection (004) may be used that does not split when rhombic distortion of the hexagonal structure takes place (Figure 3). Main parameters of diffraction peak recording: counter angle pitch was equal to  $\Delta(2\theta) = 0.02^\circ$ , and the exposure time in each point was chosen such that to achieve the sufficient statistics (maximum peak  $3\text{--}4 \cdot 10^3$ ) and was equal to 20–50 sec depending on the peak intensity.

Splitting of reflection  $\{(400) + (260)\}$  gives the distortion

$$\varepsilon_o = (a - b/\sqrt{3})/a = 2(d_1^2 - d_2^2)/(4d_1^2 - d_2^2),$$

$$(d_{1,2}^{-1} = 2 \sin(\theta_{1,2})/\lambda),$$

where  $\theta_1 = \theta_{400}$ ,  $\theta_2 = \theta_{260}$  — are the Bragg angles of the particular reflections. At  $T = 300$  K, the reflection is not split and  $d_1 = d_2$  at  $b_o = \sqrt{3}a_o$ , i.e. the sample has hexagonal structure. Thus, the phase transition temperature  $T_S$ , at which lattice symmetry decreases, is below 300 K.

During distortion, the high-angle component of the split reflection remains in place and an additional line shifted by  $\Delta(2\theta) \approx 0.2^\circ$  appears (Figure 1). Reflection with angle  $2\theta_{1,2} \approx 69^\circ$  is split in a stepwise manner at the phase transition temperature and is almost unchanged at temperature decrease up to 80 K. For the second reflection (004), the angle  $2\theta_3 \approx 41^\circ$  grows in a stepwise manner by  $\Delta(2\theta_3) \approx 0.2^\circ$  at  $T_S$  and continues growing with temperature decreasing to 80 K (Figure 2). Reflection (004) is not split and is fairly far from other reflections, therefore its profile clearly shows two-phase state, when both phases exist in a small temperature range  $\approx (5\text{--}10)$  K near  $T_S$ . Changes of lattice constants of Tm cobaltite with temperature are shown in Figure 4. For ease of comparison, relative changes of all lattice parameters  $\Delta a/a$ ,  $\Delta b/b$ ,  $\Delta c/c$  (curves 1–3), volume  $\Delta V/V = (\Delta a/a + \Delta b/b + \Delta c/c)$  (curve 4) and rhombic distortions  $\varepsilon_o = \Delta a/a - \Delta b/b$  (curve 5) are normalized to their values at  $T = 300$  K. For example,  $\Delta a/a = \Delta a(T)/a_o$  ( $\Delta a(T) = a(T) - a_o$ ;  $a_o = a(T = 300 \text{ K})$ ). The use of relative parameter changes also allow avoid the influence of possible systematic error. Relative measurement error of  $\delta a_i/a_i$  lattice parameters and rhombic deformation  $\delta \varepsilon_o/\varepsilon_o$  (which does not depend on the alignment) is equal to  $\approx 1\text{--}2 \cdot 10^{-4}$ , relative error for volume measurement composed of errors of all parameters may be considerably higher.

For quenched  $\text{TmBaCo}_4\text{O}_7$ , nontrivial behavior of  $a$  parameter is observed, which decreases with increasing

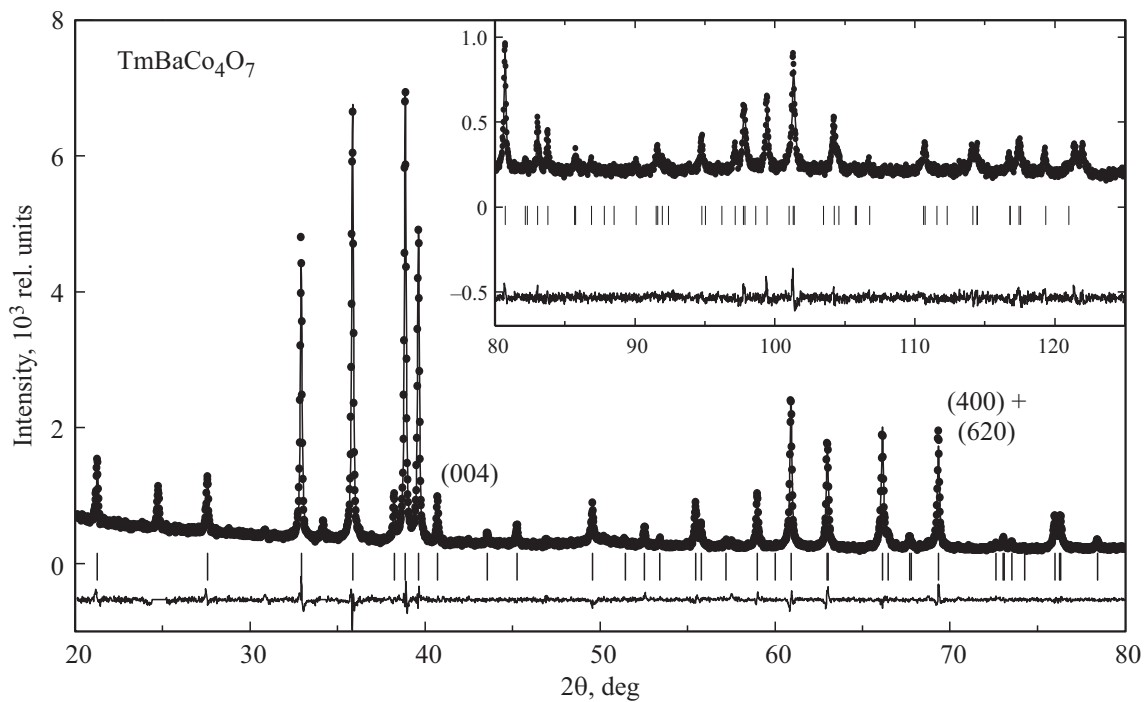


**Figure 1.** Experimental (dots) and calculated (lines) X-ray images and the difference (lines in the bottom) for annealed  $\text{TmBaCo}_4\text{O}_7$  sample with  $\text{CoK}_{\alpha 1}$ -radiation. Vertical bars show the Bragg peak positions according to the space group. The insert shows scaled up large-angle X-ray image portion.

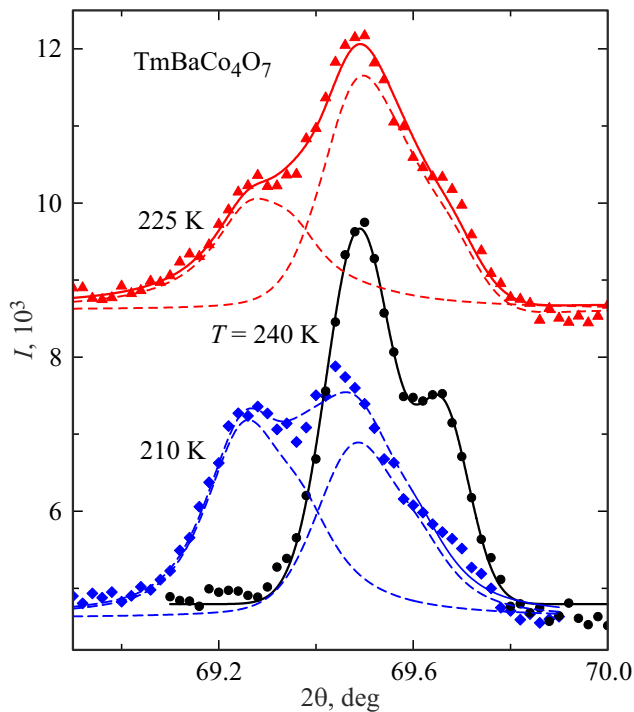


**Figure 2.** Experimental (dots) and calculated (lines) diffraction peaks  $\{(400) + (260)\}$  with  $\text{CoK}_{\alpha 1,2}$ -radiation of the stoichiometric  $\text{TmBaCo}_4\text{O}_7$  sample in the hexagonal ( $T = 240$  K) and orthorhombic ( $T = 210$  K; dashed lines — components of the peak split during distortion) phase. Reflection at 225 K corresponds to two-phase state (displaced on the  $x$  axis for ease of comparison).

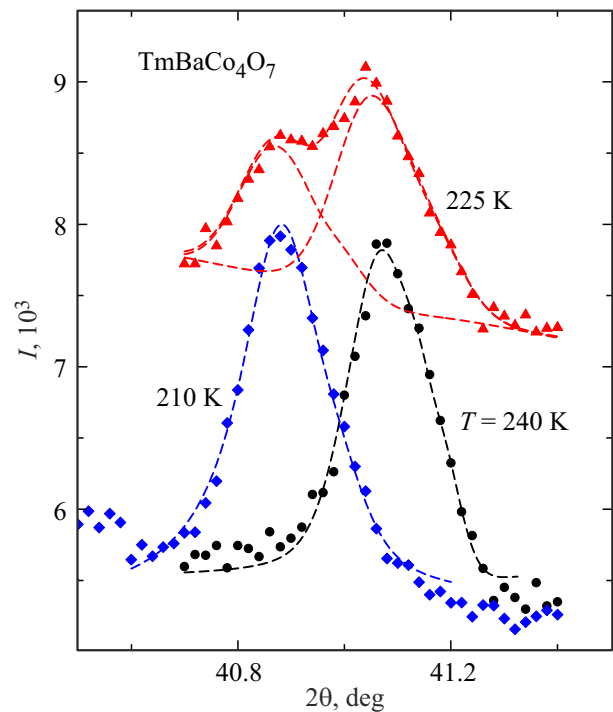


**Figure 3.** Experimental (dots) and calculated (lines) diffraction peaks (004) with  $\text{CoK}_{\alpha 1,2}$ -radiation of the stoichiometric  $\text{TmBaCo}_4\text{O}_7$  sample in the hexagonal ( $T = 240$  K) and orthorhombic ( $T = 210$  K) phase. Reflection at 225 K corresponds to two-phase state (displaced on the  $x$  axis for ease of comparison).

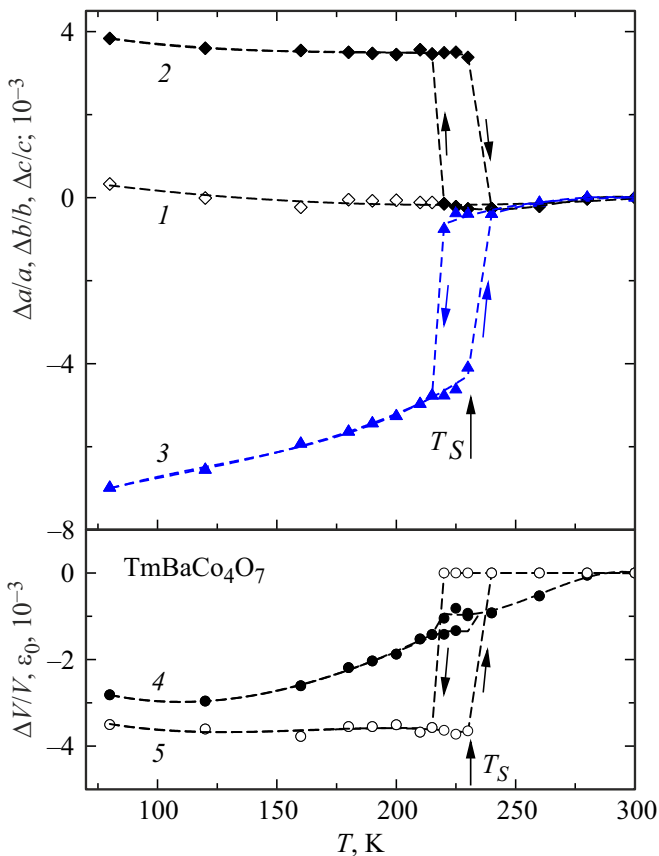


**Figure 4.** Relative changes of the lattice parameters (curve 1 —  $\Delta a/a$ , 2 —  $\Delta b/b$ , 3 —  $\Delta c/c$ ), volume  $\Delta V/V = (\Delta a/a + \Delta b/b + \Delta c/c)$  (curve 4) and degree of rhombic distortion  $\varepsilon_o = (\Delta a/a - \Delta b/b)$  (curve 5) with the temperature of the quenched  $\text{TmBaCo}_4\text{O}_7$  sample. All dependences are normalized to the parameter value at  $T = 300$  K.

temperature and has not step change during phase transition. This situation is also typical for Er cobaltite. The parameters  $b$  and  $c$  at  $T_S$  are changed stepwise ( $\Delta b/b \approx 3.5 \cdot 10^{-3}$  and  $\Delta c/c \approx -4.0 \cdot 10^{-3}$ ) resulting in the step change of  $\Delta V/V \approx -0.5 \cdot 10^{-3}$ . In the region  $T < T_S$  during heating, the parameters  $b$  and  $a$  change a little and in a similar way, while the parameter  $c$  grows. As a result, with increasing  $T$ , distortion  $\varepsilon_o$  is unchanged and has a step change  $\Delta \varepsilon_o \approx -3.5 \cdot 10^{-3}$  only in the phase transition region, whose temperature is within  $\approx 220$ – $240$  K. In the structural phase transition region, two-phase state is observed, when high- and low-temperature phases co exist at the same time, which is typical for other previously studied cobaltites [26]. It should be noted that the parameter  $c$  of  $\text{TmBaCo}_4\text{O}_7$  continues growing at a lower rate and above the phase transition up to room temperature. Thus, during heating to  $T_S$ , volume change (volumetric thermal expansion) in this compound is mainly attributable to the increase of the parameter  $c$ , and after  $T_S$  this change is due to the growth of all lattice parameters.

### 3.2. Elastic properties

Elastic moduli are very sensitive to phase transitions of different nature [30] and their temperature dependences allow to determine both the transition temperature and the effect of various factors on the transition. Temperature dependences of the Young's modulus  $E(T)$  and internal friction  $q^{-1}(T)$  for  $\text{TmBaCo}_4\text{O}_7$  quenched from  $900$ – $950^\circ\text{C}$  will be discussed below. Temperature dependences  $\Delta E(T)/E_0$  show different behavior for different compounds of the family [37,38].

For the ease of comparison with previously studied compounds, the Figure shows relative changes of the Young's modulus with temperature:  $\Delta E(T)/E_0$  ( $\Delta E(T) = E(T) - E_0$ ;  $E_0 = E(T = 300 \text{ K})$ ) normalized to  $E_0$  at  $T = 300$  K. Structural phase transition in the annealed  $\text{TmBaCo}_4\text{O}_7$  sample causes softening of the Young's modulus with temperature decrease starting at a temperature much higher than the phase transition temperature (Figure 5) and is followed by an anomaly in curve  $\Delta E(T)/E_0$  in the structural transition region near  $T_S = 220$  K. Thus, the presence of softening and a pronounced minimum on the curve  $\Delta E(T)/E_0$  with decreasing temperature are indicative of the phase transition. In addition, the structural transition is followed by significant hysteresis, when the curve near  $T_S$  corresponding to the sample cooling goes below the curve corresponding volume to heating.

To determine the structural phase transition temperature and hysteresis, we used the temperature dependences of

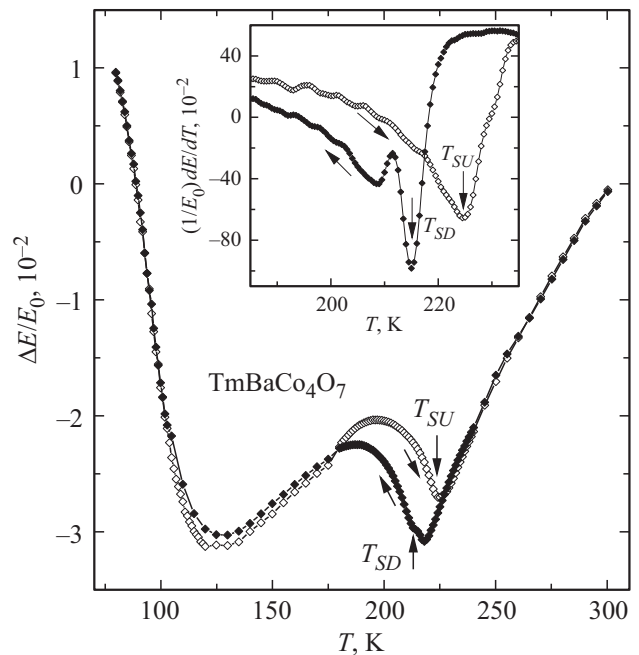


**Figure 5.** Dependence of the relative Young's modulus  $\Delta E(T)/E_0$  on temperature for the quenched  $\text{TmBaCo}_4\text{O}_7$  sample during heating (light dots) and cooling (dark dots). The insert shows the dependence of the temperature derivative of the Young's modulus  $(1/E_0)dE/dT$  in the structural transition region.

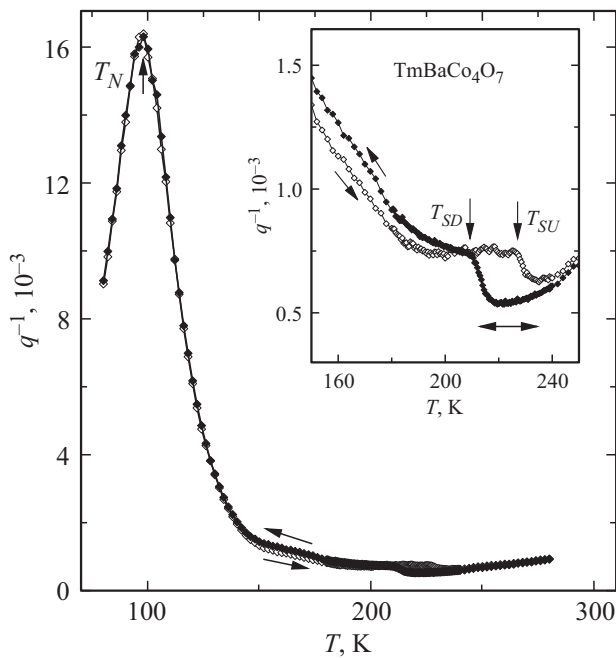


**Figure 6.** Temperature dependence of the internal friction  $q^{-1}(T)$  for the quenched  $\text{TmBaCo}_4\text{O}_7$  sample during heating (light dots) and cooling (dark dots). The insert shows the scaled up structural transition region.

derivative  $(1/E_0)dE(T)/dT$ , where the transition temperature corresponded to the minimum derivative (insert in Figure 5). The structural transition temperature determined by the Young's modulus derivative extrema  $(1/E_0)dE/dT$  is equal to  $T_{SU} \approx 225$  K and  $T_{SD} \approx 215$  K during heating and cooling, respectively, i.e. the transition is followed by the temperature hysteresis about 10 K. It should be noted that a more prolonged two-step transition takes place during cooling, while the transition during heating is more abrupt. Such feature of the Young's modulus irregularities was observed before during the martensitic transformation in shape memory alloys [39].

The internal friction dependence  $q^{-1}(T)$  (Figure 6) shows steps at temperatures close to the transition temperatures  $T_{SU}$ ,  $T_{SD}$  found in the curves  $\Delta E(T)/E_0$ . Steps in the curves  $q^{-1}(T)$  are believed to correspond to the diffused or „smoothed“  $\lambda$  — anomalies for the perfect example. And the top of the step in  $q^{-1}(T)$  („diffused“  $\lambda$  — anomalies) is by 5 K lower than the minimum Young's modulus derivative  $(1/E_0)dE(T)/dT$ .

Structure distortion of the stoichiometric samples  $\text{RBaCo}_4\text{O}_{7+x}$  due to the structural transition results in frustration release, which shall promote the establishment of long-range magnetic order in the cobalt subsystem. Actually, for the distorted and near-stoichiometric  $\text{YBaCo}_4\text{O}_7$  samples, step  $\Delta E/E_0$  (or peak in the derivative  $(1/E_0)dE/dT$ ) and high peak in the dependence  $q^{-1}(T)$  are observed in the phase transition region  $T_N \sim 105$  K. For stoichiometric Er cobaltite, pronounced anomalies of the elastic properties

are also observed in the magnetic phase transition region in the Co subsystem. The stoichiometric  $\text{TmBaCo}_4\text{O}_7$  sample was also expected to exhibit clearly pronounced magnetic transition followed by the elastic property anomalies in the  $T_N$  region. Detailed investigations of  $\text{TmBaCo}_4\text{O}_7$  show the absence of any anomalies in the temperature dependence of the Young's modulus in the  $T_N \sim 100$  K region, where magnetic phase transition is expected. However, for the  $\text{TmBaCo}_4\text{O}_7$  studied sample, there is a rather large temperature trend  $\Delta E(T)/E_0 \approx 4 \cdot 10^{-2}$  within the range of 80–120 K, against which it is difficult to record small anomalies  $\delta E(T_N)/E_0 < 10^{-2}$ . However, on the internal friction curve  $q^{-1}(T)$ , a pronounced peak  $\approx 16 \cdot 10^{-3}$  is observed at  $T_{\max} = 96$  K, which is the same during heating and cooling and often accompanying the magnetic phase transition. Thus, the long-range magnetic order is probably not achieved in the studied sample and the presence of developed short-range order may be only suggested.

#### 4. Conclusion

In frustrated and low-dimensional systems, the development of the long-range magnetic order depends on various weak interactions and perturbations such as small structure distortion, magnetic anisotropy induced by the RE ion, disorder of different nature, etc. A minor distortion of structure in stoichiometric RE cobaltites removes the frustration of exchange interactions due to the structural transition promoting the development of a long-range magnetic order in the Co subsystem below  $T_S$  [23,25]. Actually, for the distorted and near-stoichiometric  $\text{YBaCo}_4\text{O}_7$  samples, step  $\Delta E/E_0$  (or peak in the derivative  $(E_0^{-1})dE/dT$ ) and high peak on the dependence  $q^{-1}(T)$  are observed in the phase transition region  $T_N \sim 105$  K. Nonstoichiometric compound structures remain undistorted and the frustrations are maintained in the system. Thus, with decreasing temperature the short-range magnetic order gradually develops, where the correlation length does not achieve the crystallite sizes.

For the stoichiometric  $\text{RBaCo}_4\text{O}_7$  cobaltites with Y, Ho, Er ions (unlike Dy cobaltite), the temperature dependences of the Young's modulus and internal friction coefficient have common patterns [34]. Similar elastic anomalies of this cobaltites suggest that magnetic behavior of their cobalt subsystem is the same. Step in the  $T_N$  region varies a little for stoichiometric RE cobaltites and the steps for nonstoichiometric compounds are diffused and decrease in value (anomalies often appear only on the derivative  $(1/E_0)dE/dT$ ).

According to the study, the stoichiometric Tm cobaltite behavior shows considerable difference. The stoichiometric  $\text{TmBaCo}_4\text{O}_7$  sample, like the Y equivalent, demonstrates the structure distortion below  $T_S = 220$  K. According to X-ray examinations, the structure distortion of the  $\text{TmBaCo}_4\text{O}_7$  sample is similar during transition: the parameter  $\Delta a/a$  does not demonstrate any features, the parameters  $b$  and  $c$  undergo steps of different signs and different magnitudes

resulting in a change of the ratio  $c/a_{av}$  for the structure and a volume step of  $\Delta V/V \sim -1 \cdot 10^{-3}$ . Also, similar anomalies are observed for structure parameters of the stoichiometric  $\text{YBaCo}_4\text{O}_7$  sample. However, for  $\text{TmBaCo}_4\text{O}_7$ , there is almost no anomaly at  $T_N \approx 105$  K either in the elastic modulus dependence  $\Delta E/E(T)$  or in its derivative. Only in the internal friction curve  $q^{-1}(T)$ , a pronounced peak  $\approx 16 \cdot 10^{-3}$  at  $T_{\max} = 96$  K is observed, which may be associated with the developed short-range order.

Thus, the phase transition nature and various physical properties in the layered  $\text{RBaCo}_4\text{O}_{7+x}$  cobaltites depend not only on the structure distortion attributed to the excess oxygen, but probably also on the magnitude and sign of the magnetic anisotropy induced by the RE subsystem. To our opinion, further investigation of layered cobaltites with other RE ions having different magnitudes and signs of magnetic anisotropy is of interest.

### Conflict of interest

The authors declare that they have no conflict of interest.

### References

- [1] P. Schiffer, A.P. Ramirez. *Comm. Condens. Matter Phys.* **18**, 1, 21 (1996).
- [2] M.J. Harris, M.P. Zinkin. *Mod. Phys. Lett. B* **10**, 10, 417 (1996).
- [3] J.N. Reimers, A.J. Berlinsky. *Phys. Rev. B* **48**, 13, 9539 (1993).
- [4] P. Lecheminant, B. Bernu, C. Lhuillier, L. Pierre, P. Sindzingre. *Phys. Rev. B* **56**, 5, 2521 (1997).
- [5] L.C. Chapon, P.G. Radaelli, H. Zheng, J.F. Mitchell. *Phys. Rev. B* **74**, 17, 172401 (2006).
- [6] P. Manuel, L.C. Chapon, P.G. Radaelli, H. Zheng, J.F. Mitchell. *Phys. Rev. Lett.* **103**, 3, 037202 (2009).
- [7] W. Schweika, M. Valldor, P. Lemmens. *Phys. Rev. Lett.* **98**, 6, 067201 (2007).
- [8] V. Caignaert, V. Pralong, A. Maignan, B. Raveau. *Solid State Commun.* **149**, 11–12, 453 (2009).
- [9] V. Caignaert, V. Pralong, V. Hardy, C. Ritter, B. Raveau. *Phys. Rev. B* **81**, 9, 094417 (2010).
- [10] K. Singh, V. Caignaert, L.C. Chapon, V. Pralong, B. Raveau, A. Maignan. *Phys. Rev. B* **86**, 2, 024410 (2012).
- [11] M. Valldor, N. Hollmann, J. Hemberger, J.A. Mydosh. *Phys. Rev. B* **78**, 2, 024408 (2008).
- [12] E.V. Tsipis, V.V. Kharton, J.R. Frade, P.J. Nuñez. *Solid State Electrochem.* **9**, 547 (2005).
- [13] D.D. Khalyavin, P. Manuel, B. Ouladdiaf, A. Huq, P.W. Stephens, H. Zheng, J.F. Mitchell, L.C. Chapon. *Phys. Rev. B* **83**, 9, 094412 (2011).
- [14] M. Karppinen, H. Yamauchi, S. Otani, T. Fujita, T. Motohashi, Y.H. Huang, M. Valkeapää, H. Fjellvag. *Chem. Mater.* **18**, 2, 490 (2006).
- [15] S. Kadota, M. Karppinen, T. Motohashi, H. Yamauchi. *Chem. Mater.* **20**, 20, 6378 (2008).
- [16] E.V. Tsipis, D.D. Khalyavin, S.V. Shiryayev, K.S. Redkina, P. Nuñez. *Mater. Chem. Phys.* **92**, 1, 33 (2005).
- [17] S. Rasanen, H. Yamauchi, M. Karppinen. *Chem. Lett.* **37**, 6, 63 (2008).
- [18] E.A. Juarez-Arellano, A. Friedrich, D.J. Wilson, L. Wiehl, W. Morgenroth, B. Winkler, M. Avdeev, R.B. Macquart, C.D. Ling. *Phys. Rev. B* **79**, 6, 064109 (2009).
- [19] E.V. Tsipis, J.C. Waerenborgh, M. Avdeev, V.V. Kharton. *J. Solid State Chem.* **182**, 3, 640 (2009).
- [20] L.P. Kozeeva, M.Yu. Kameneva, A.I. Smolentsev, V.S. Danilovich, N.V. Podberezskaya. *ZhSKh* **49**, 4, 6 (1108). (in Russian).
- [21] A. Huq, J.F. Mitchell, H. Zheng, L.C. Chapon, P.G. Radaelli, K.S. Knight, P.W. Stephens. *J. Solid State Chem.* **179**, 4, 1136 (2006).
- [22] D.D. Khalyavin, L.C. Chapon, P.G. Radaelli, H. Zheng, J.F. Mitchell. *Phys. Rev. B* **80**, 14, 144107 (2009).
- [23] M. Markina, A.N. Vasiliev, N. Nakayama, T. Mizota, Y. Yeda. *J. Magn. Magn. Mater.* **322**, 9–12, 1249 (2010).
- [24] M. Valldor, Y. Sanders, W. Schweika. *J. Phys.: Conf. Ser.* **145**, 1, 012076 (2009).
- [25] Z.A. Kazey, V.V. Snegiryov, L.P. Kozeeva, M.Yu. Kameneva, A.N. Lavrov. *ZhETF* **153**, 5, 782 (2018). (in Russian).
- [26] Z.A. Kazey, V.V. Snegiryov, M.S. Stolyarenko. *ZhETF* **160**, 5, 689 (2021). (in Russian).
- [27] N. Nakayama, T. Mizota, Y. Ueda, A.N. Sokolov, A.N. Vasiliev. *J. Magn. Magn. Mater.* **300**, 1, 98 (2006).
- [28] V. Caignaert, A. Maignan, K. Singh, C. Simon, V. Pralong, B. Raveau, J.F. Mitchell, H. Zheng, A. Huq, L.C. Chapon. *Phys. Rev. B* **88**, 17, 174403, (2013).
- [29] A. Maignan, V. Caignaert, D. Pelloquin, S. Hébert, V. Pralong, J. Hejtmanek, D. Khomskii. *Phys. Rev. B* **74**, 16, 165110 (2006).
- [30] Z.A. Kazey, V.V. Snegiryov, A.S. Andreenko, L.P. Kozeeva. *ZhETF* **140**, 2, 282 (2011). (in Russian).
- [31] M.J.R. Hoch, P.L. Kuhns, S. Yuan, T. Besara, J.B. Whalen, T. Siegrist, A.P. Reyes, J.S. Brooks, H. Zheng, J.F. Mitchell. *Phys. Rev. B* **87**, 6, 064419 (2013).
- [32] M. Soda, Y. Yasui, T. Moyoshi, M. Sato, N. Igawa, K. Kakurai. *J. Phys. Soc. Jpn.* **75**, 5, 054707 (2006).
- [33] Z.A. Kazey, V.V. Snegiryov, M.S. Stolyarenko, K.S. Pigalsky, L.P. Kozeeva, M.Yu. Kameneva, A.N. Lavrov. *FTT* **60**, 12, 2459 (2018). (in Russian).
- [34] Z.A. Kazey, V.V. Snegiryov, L.P. Kozeeva, M.Yu. Kameneva. *ZhETF* **149**, 1, 155 (2016). (in Russian).
- [35] Z.A. Kazey, V.V. Snegiryov, M.S. Stolyarenko. *Pis'ma v ZhETF* **112**, 3, 189 (2020). (in Russian).
- [36] L.P. Kozeeva, M.Yu. Kameneva, A.N. Lavrov, N.V. Podberezskaya. *Neorgan. materialy* **49**, 6, 668 (2013). (in Russian).
- [37] Z.A. Kazei, V.V. Snegirev, A.A. Andreenko, L.P. Kozeeva, M.Yu. Kameneva. *Solid State Phenomena* **233**, 145 (2015).
- [38] Z.A. Kazei, V.V. Snegirev, L.P. Kozeeva, M.Yu. Kameneva. *Solid State Phenomena* **190**, 482 (2012).
- [39] Z.A. Kazey, V.V. Snegiryov. *FTT* **61**, 7, 1223 (2019). (in Russian).

Translated by E.Ilyinskaya